Journal of Sound and Vibration (2000) **238**(4), 547–574
doi:10.1006/jsvi.1999.3132, available online at http://www.idealibrary.com on IDEAL®

MODELLING LIQUID–STRUCTURE INTERACTIONS WITHIN THE FRAMEWORK OF STATISTICAL ENERGY ANALYSIS

M. LIU

Department of Engineering Science, University of Oxford, Parks Road, Oxford, OX1 3PJ

A. J. KEANE

School of Engineering Sciences, University of Southampton, Highfield, Southampton, SO17 1BJ.
E-mail: ajk@soton.ac.uk

AND

R. EATOCK TAYLOR

Department of Engineering Science, University of Oxford, Parks Road, Oxford, OX1 3PJ

(*Received* 2 *December* 1998, *and in final form* 3 *December* 1999)

This paper presents some work undertaken as part of a managed programme in statistical energy analysis (SEA) and its application to problems with liquid loadings. A study of vibrations involving a coupled fluid–structural system has been carried out and the results from this used to examine aspects of statistical energy analysis modelling in this context. The study involved a series of numerical analyses undertaken using the finite element method. In dealing with coupled systems consisting of fluids and structures two approaches were employed: direct FE models using elements formulated for acoustic and solid domains, and modal representation of the solids in the coupled models. Dynamic response analysis was then performed for the combined models. A wide spectrum of energy levels was obtained when the models were subjected to various types of loading. Based on these numerical analysis results a number of SEA models were established with different topological interconnections. These were then used to make forced response predictions that could be compared with full finite element calculations. Various test case results are presented and associated conclusions drawn from the study. It is shown that the more complex SEA models do not necessarily give improved accuracy.

1. INTRODUCTION

The role of computational structural analysis has been fundamental to the design of most modern ships and offshore marine structures. It is now common place to design and build vast concrete and steel structures that will withstand the worst that nature can impart to them. However, it is inevitable that, as current problems are tackled and brought under control, higher standards are desired by both operators and regulators. Initially, structural integrity was the main design criterion; now this is considered along-side reduced through-life cost, ease of maintenance, higher standards of habitability, etc. One of the consequences of this shift in emphasis is the need for new design and analysis tools to be brought on stream to deal with problems that have, until recently, not been seen as high priorities.

0022-460X/00/490547 + 28 $35.00/0

One area that has become increasingly important in all engineering spheres is that of noise and vibration control. Noise standards are becoming more stringent and structural vibration can lead to rapid fatigue failures, particularly in light-weight structures. This topic has been the subject of research for many years and a number of palliative techniques such as vibration isolation mountings, acoustic claddings, etc., are routinely used in engineering structures. Nonetheless, most such techniques are rather *ad hoc* in nature and the application of classical vibration theory to real problems in engineering is never simple or wholly satisfying. Difficulties arise for a number of reasons; not least among these are the problems involved in solving the resulting differential equations of motion or, indeed, in providing an adequate model in the first place. These may be compounded by the lack of a detailed description during the early stages of design, or by the inaccuracies inherent in manufacture or construction (leading to the study of statistical models).

It would clearly be desirable to be able to calculate the effects of various noise control measures during the design process by assessing the paths that vibrational energy takes when flowing around a structure and also the predominant modes of energy transfer. Armed with such information it would then be possible to take appropriate steps.

Unfortunately, most of the structures used in modern engineering design are quite complex and, even at low to medium frequencies say (50–1000 Hz), their acoustic behaviour cannot be dissociated from their structural dynamics, particularly when they incorporate or must interact with liquids. These frequency ranges are not readily amenable to analysis by using finite elements (FE) or standard acoustic methods. FE analysis, for instance, requires large, fast computational facilities in order to deal with the mathematical models representing very detailed idealizations of the physical structures. Even so it is generally not practicable to predict the detailed vibrational behaviour of such structures at frequencies beyond the first 20 or so vibrational modes. The high-frequency modes are more prone to errors than those of lower order, and even mis-sequenced. At high modal numbers the error in the calculation of the modal frequency is often greater than the difference between successive modes, and so the modes do not appear in their correct order, especially when modal density increases [1]. In such circumstances other methods such as statistical energy analysis (SEA) may be more appropriate. As a tool for making assessments of vibrational behaviour in terms of energy flow, SEA can also be used to process data obtained by FE analysis and to interpret results which otherwise are less useful due to computational shortcomings and model inadequacies.

Initially conceived in the early 1960s, SEA has been developed mainly in the context of light-weight aerospace structures where engineers sought new methods for dealing with the problem of predicting the responses of launcher and payload structures to rocket noise at launch. Statistical concepts and models of dynamic behaviour which had been exploited for many years in the analysis of sound fields were extended and adapted to structural systems. System parameters were expressed in probabilistic terms, and the objective of an analysis was seen to be the prediction of the ensemble-average behaviour of sets of grossly similar realizations of an archetypal system (such as the products of an industrial production line). System response to vibrational inputs was characterized by averaged vibrational energy; energy flow between coupled sub-systems was expressed in terms of energy transfer coefficients; and vibrational energy distribution was determined from power balance equations.

Since that time, SEA has undergone relatively little rigorous theoretical development, but the basic results for simple idealized systems have been tested against those from alternative, deterministic approaches which may be implemented because of the simplicity of the models. SEA predictions have also been tested against experimental results, but, because of the large amount of poorly, and even misleadingly, presented information, it is extremely

difficult to draw reliable conclusions from some of these. However, it can be confidently stated that when properly applied, SEA concepts have provided a very useful framework on which to design experiments and generate empirical data. In fact, on the basis of such data, both the European Space Agency and NASA routinely use SEA methods to predict the response of spacecraft to in-flight vibrational inputs.

As a result, much SEA research has examined the behaviour of simple archetypal systems such as rectangular panels joined to beams and such like. The majority of this work has concentrated on the kind of joints and structures encountered in the aerospace industry, with relatively little work on heavier structures or those involving liquids [2]. Consequently, before applying SEA to fluid-loaded structures, it would appear prudent to extend this work by studying some typical configurations. One such area of structural design, where vibrational damage is a serious risk (because of fatigue failure), concerns the large diameter oil and water pipework runs commonly found on ships and offshore rigs.

The objective of the current study is therefore two-fold; to improve the state of knowledge in this area given that relatively little work has been carried out on mid-frequency vibration problems involving structures interacting with liquids, and to develop and apply SEA methodology in this context.

Large diameter pipework systems were identified as being an interesting case for examination since there have been some problems with such systems on offshore installations. In the frequency ranges that might be considered, strong coupling between the enclosed liquid and the structure is to be expected. Such coupling may result in behaviour which is qualitatively different from that of the structure vibrating in say air, for which the coupling is relatively weak, and therefore this might require a different approach to the SEA modelling of such problems.

2. FINITE ELEMENT MODELLING

Before building any theoretically based SEA models it is often first necessary to carry out detailed numerical analyses on the problems of interest (here liquid-filled pipework systems). In this study, these analyses have been carried out by using FE methods and they form the datum against which the SEA models have been tested. The use of FE is necessary because no closed-form solutions are available for the problems of interest, which is not surprising given that combined noise transmission and fluid–structure interactions are of concern. The FE analyses are used to identify various sub-system loss and coupling loss coefficients for the SEA models and also to test these models. The basic system considered here consists of three sections of pipework comprising two straight sections of cylindrical shell joined by a 90° bend all being filled with water.

2.1. SYSTEM PROPERTIES

The pipework model used here has the following dimensions: axial lengths of the straight sections $L = 3{\cdot}0$ m; centreline radius of the bend $R = 0{\cdot}5$ m; diameter $2a = 0{\cdot}15$ m and, wall thickness $h = 0{\cdot}005$ m. The pipe system is made of steel with Young's modulus $E = 206{\cdot}8 \times 10^9$ Pa and the Poisson ratio $\nu = 0{\cdot}29$; shear modulus $G = 80{\cdot}16 \times 10^9$ Pa; density $\rho = 7{\cdot}82 \times 10^3$ kg. Rayleigh damping for the cylindrical shell sections is taken as $\alpha = 0$, $\beta = 7{\cdot}668E - 7$ and for the bend as $\alpha = 0$, $\beta = 1{\cdot}5336E - 6$ kg. The properties of water are taken as density $\rho_f = 1{\cdot}0 \times 10^3$ kg m^3 and bulk modulus $E_f = 2{\cdot}1 \times 10^9$ Pa. It is noted that these parameters are representative of typical water-main pipe runs on many

offshore structures. They lead to the following properties for the unloaded straight sections of pipe: a first natural frequency of 47 Hz, a ring frequency of 540 Hz and the first 50 modes spanning a range of 1690 Hz; i.e., a modal density of 0·0006 modes/Hz for the dry shell.

2.2. FINITE ELEMENT FORMULATION

Three types of elements are utilized in the FE models: i.e., shell elements, acoustic elements and interface elements. Classical shell theories abound [3–5]; however, when a closed-form solution is not available FE methods must be adopted. Recently, considerable effort has been made in developing new finite element methods for dealing with coupled systems in the context of SEA, notably by Finnveden [6, 7]. The spectrum elements developed there have improved our understanding and capability in dealing with fluid-filled pipe systems. However, spectrum elements based on closed-form solutions of asymmetrical systems have not yet been extended to analyzing more complex system configurations, such as those with bends. Here, therefore, more traditional finite element methods are adopted.

For the FE analysis a four-noded shell element was generally used for the results obtained below, due to its simplicity and ease of coupling with fluids. However, in order to examine the accuracy of the FE analysis models, parabolic quadrilateral shell element models were also studied, all by using the ABAQUS code [8].

Eight-noded acoustic elements were formulated and used for modelling the fluid, assuming it to be compressible but undergoing only small pressure variations.

The discrete equations for shells and fluids are

$$M\ddot{u} + Ku = F + \gamma A^{\mathrm{T}} p, \qquad M_f \ddot{p} + K_f p = P - A\ddot{u}, \tag{1}$$

where M, K, M_f, K_f, u, p, F and P are solid mass and stiffness matrices, fluid mass and stiffness matrices (actually relating to the fluid strain energy and kinetic energy respectively), solid displacement and fluid pressure, and external loadings on solid and fluid, respectively, and γ, A are, respectively, a scalar and a rectangular matrix built according to interface elements.

Associated damping can be included according to various damping schemes such as structural damping for solids or volumetric drag coefficient for the fluid. Here, proportional Rayleigh damping of the form $[C] = \alpha[M] + \beta[K]$ was adopted for the shells with $\alpha = 0$, and β varying from section to section.

With the inclusion of damping the steady state equations at frequency ω can be recast as

$$\left(-\omega^2 \begin{bmatrix} M & 0 \\ A & M_f \end{bmatrix} + \mathrm{i}\omega \begin{bmatrix} \mathrm{C} & 0 \\ 0 & \mathrm{C}_f \end{bmatrix} + \begin{bmatrix} K & -\gamma A^{\mathrm{T}} \\ 0 & K_f \end{bmatrix} \right) \begin{Bmatrix} \bar{u} \\ \bar{p} \end{Bmatrix} = \begin{Bmatrix} \bar{F} \\ \bar{P} \end{Bmatrix}, \tag{2}$$

where C and C_f are damping matrices and C_f is related to the volumetric drag coefficient r. The overbar indicates the complex amplitude of the corresponding time-harmonic variable.

Interface elements are required in the ABAQUS model to couple the acoustic elements to the structural models due to the different types of physical variables involved (pressure and displacement respectively). These interface elements couple the pressure that the acoustic medium applies on the structural surface to the acceleration of that surface, in the direction normal to the surface. The interface element is created such that the side of the surface pointing into the fluid is defined by the right-hand rule from the order of the nodes on the element. It then shares common nodes with one surface of the shell element and one surface of the acoustic element to link the shell and fluid models. In this way, displacement compatibility can be maintained with the structural model and pressure field compatibility

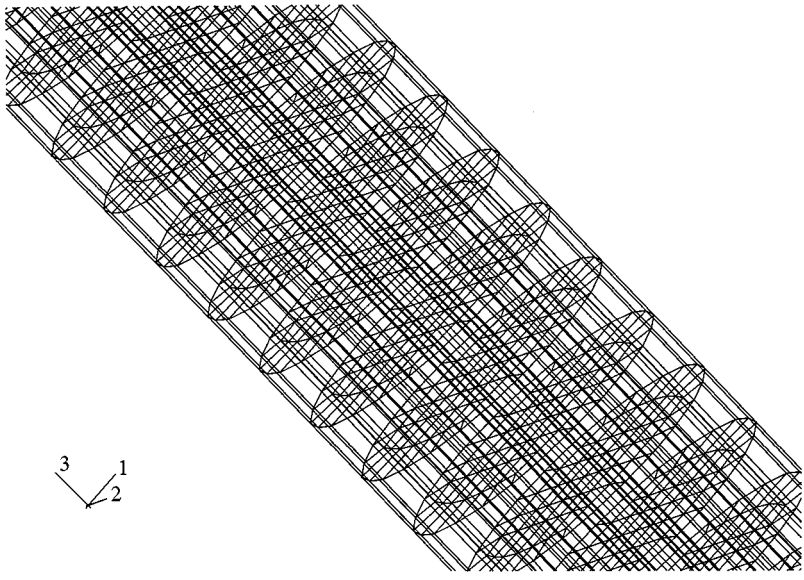

Figure 1. A section of the FE model consisting in total of 5888 shell, 5888 acoustic and 11 100 interface elements.

with the acoustic model. Note, however, that the sequence of the nodes differs from that of the shell or acoustic elements.

Since symmetry is then lost from the assembled system equations, the use of efficient solution algorithms becomes critical (n.b., symmetry of the coupled equations may be recovered [9, 10] but only at the cost of destroying the FE bandwidth and sparsity). Here positive (semi-)definite matrices no longer result and this restricts the type of algorithms that may be used for the numerical analysis. As a result, few commercial packages can be executed with optimal solution algorithms when dealing with coupled problems of this class.

Of course, if the fluid is incompressible, then $[K_f] = 0$, and either u or p in equation (2) can be eliminated exactly by using Guyan static reduction. Standard symmetrical forms are then obtainable [9], leading to a simple added mass model of the coupled systems. For the more general compressible case of interest here, Irons [10] proposed the application of Cholesky decomposition in order to achieve a standard symmetrical form and the efficiency of this approach was then improved by MacNeal [11], who introduced approximate modal transformation and reduction techniques. However, in the ABAQUS package only a direct integration method is provided for frequency response analysis of such coupled systems.

2.3. DYNAMIC ANALYSIS

A dynamic analysis was performed using the element types outlined above: part of the FE model illustrating the mesh density is shown in Figure 1. The details of the FE model are as follows: 82 026 degrees of freedom (d.o.f.s), consisting of 5888 shell elements, 5888 interface elements and 11 100 acoustic elements with translational restraints at the extreme pipe ends (simply supported). A rigid boundary condition was employed for the fluid at the pipe ends. Eigenanalysis was undertaken and frequency responses obtained for the system when subject to various point harmonic excitations of unit constant amplitude force and pressure (force N, pressure Pa).

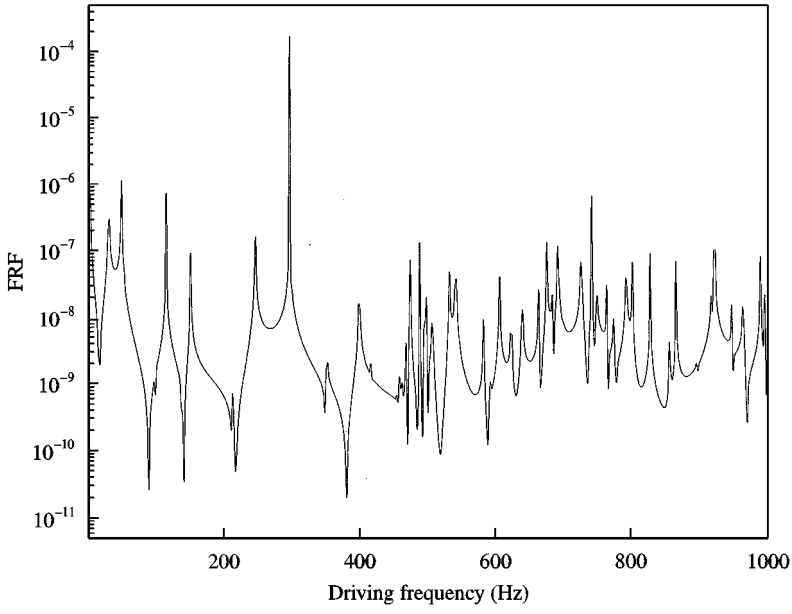

Figure 2. Frequency response function (FRF, displacement/force) for point bending loading.

The dry modes for the system (i.e., without the presence of fluid loading) were extracted first. In this case $\gamma = 0$ is assumed in equation (1). Analysis methods based on the eigenmodes are usually relatively cost effective, providing insight into the structure's dynamic behaviour that is not otherwise available. The modes are also the main ingredient needed when constructing modal representations to characterize SEA sub-systems. They can also be used for evaluating energy by modal decomposition and summation.

The full, fluid-loaded FE models were used next to obtain dynamic responses. Figure 2 shows a typical frequency response function (FRF, displacement/force) obtained over the frequency range up to 1000 Hz, for point bending loading.

In addition to the direct FE models, a modal representation model was created using the modes obtained for the dry analysis and nodal pressure co-ordinates for the fluid. In this approach, higher ordered modes are truncated and those retained are included in the fluid-loaded model by using multi-point modal constraint equations (i.e., by using a set of constraint equations, expressed in terms of the shell modal co-ordinates, superposed at the interface to set-up a modal synthesis model of the coupled system). In this way, the fluid displacement at the boundary in contact with shell is expressed by expanding the retained dry modes. This effectively translates the problem to modal co-ordinates. The equations of motion for the structure are transformed in terms of modal mass, stiffness and damping. The number of d.o.f.s is thus reduced and numerical analysis of the model requires less-computing resources, although it does require additional time to process the constraint equations.

Convergence of this model was investigated by incorporating different numbers of modes. As expected, the FRF converges when the number of modes in the model increases (see Figure 3) which shows a typical set of FRFs obtained for the model when using 5, 10, 15, 25 and 35 modes respectively. Note that the number of resonant peaks here does not tally directly with the mode count because the forcing used to construct this particular graph does not excite all the mode types: other, similar, plots show different numbers and locations of resonant peaks but equivalent convergence properties.

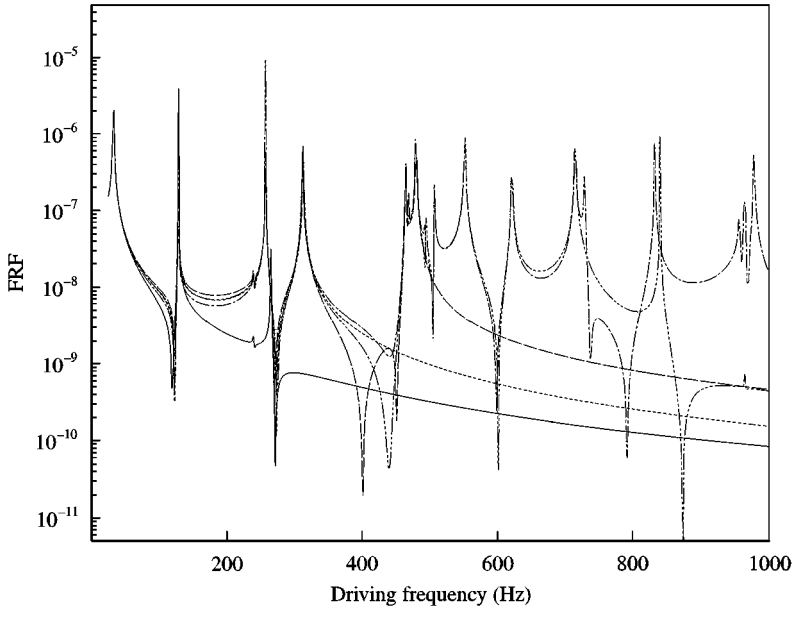

Figure 3. Frequency response functions (FRFs) obtained for the modal model using 5, 10, 15, 25, and 35 modes, respectively, for the straight section of pipework: —— 5 modes; ----- 10 modes; — — — 15 modes; — --- — --- 25 modes; — - — - 35 modes.

3. STATISTICAL ENERGY ANALYSIS

The application of SEA consists of breaking up a large system into a number of sub-systems and setting up vibrational power balance equations for each sub-system following an analogy to thermal problems dealing with heat flow: e.g., the temperature distribution for a given system can be determined if the thermal properties, input power, transfer coefficients between sub-systems and from sub-systems to their surroundings are known. Conversely, should the temperatures, input power and thermal properties be available, the heat transfer coefficients can be deduced. An understanding of the couplings between the sub-systems and the losses within them is thus central to this approach.

In SEA, coupling loss factors are used to determine the energy flow between sub-systems and loss factors to represent power dissipation associated with sub-system damping. For some simple scenarios the coupling loss factors can be theoretically calculated: i.e., by using (a) the modal approach; (b) the wave approach or (c) the wave intensity approach [2]. However, for most practical problems, they cannot be calculated directly and must be identified by empirical means or specified on the basis of past practice. Coupling loss factors can also be found by using experimental methods, by matrix fitting to measured data. Such methods are well documented, see for example references [12–15] which deal with the determination of these factors by using the power injection method.

Here, the results of a series of FE analyses are treated as experimental data and then the power injection method is used to extract loss factors and coupling loss factors from these calculations. These may then be tested by applying the derived SEA models to further test cases which may also be analyzed by using the FE approach: i.e., two sets of FE results are used, one for building the SEA models and one for validating them. This approach does, of course, treat the FE data as being correct for all the cases modelled.

3.1. KINETIC ENERGY IN SUB-SYSTEMS

In SEA the sub-systems are assumed to be resonant, linear and undergoing harmonic motion, so that the vibrational energies can be represented by either the maximum potential or kinetic energies.

The sub-system kinetic energies can be approximated by $E_i = \frac{1}{2} M_i v_i^2$ for solids and $E_i = \frac{1}{2} V_i p_i^2 / \rho_f c^2$ for fluids. Here M_i is the mass, v_i^2 is the space-averaged mean-square velocity at frequency ω, V_i is the volume of the fluid domain, ρ_f is the density of the fluid medium, c is the speed of sound in the medium and p_i^2 is the spatial-averaged mean-square pressure in the frequency band of centre frequency ω_c, where the parameters refer to sub-system i and are appropriately used for vibratory and acoustic systems.

For the fluid domain, the displacement potential satisfies

$$\nabla^2 \Phi = -(\omega^2/c^2)\,\Phi, \tag{3}$$

where Φ is the potential function for the fluid, and c is the speed of the sound in the fluid. The velocity potential Ψ is related to the displacement potential by $\Psi = \mathrm{i}\omega\Phi \mathrm{e}^{\mathrm{i}\omega t}$.

The fluid boundary is denoted by $B = B_s + B_r + B_f$, representing the fluid boundary in contact with the solid shell, rigid boundary and free surface respectively. The corresponding boundary conditions are, therefore given by

$$\partial\Phi/\partial n = \mathbf{u}\cdot\mathbf{n} \quad \text{on } B_s, \qquad \partial\Phi/\partial n = 0 \quad \text{on } B_r, \qquad g\partial\Phi/\partial n = \omega^2\Phi \quad \text{on } B_f, \tag{4}$$

where $\mathbf{n}$ is the normal vector to the boundary surface with its positive direction pointing outwards into the fluid domain and g is the acceleration due to gravity.

For the complete coupled fluid–structure system, the potential energy may then be written as

$$U_i = \frac{1}{2}\sum_{e=1}^{N_e} \mathbf{u}^{e^{\mathrm{T}}} K^e \mathbf{u}^e + \frac{1}{2}\rho_f c^2 \iiint_V \left[\left(\frac{\partial^2\Phi}{\partial x^2}\right)^2 + \left(\frac{\partial^2\Phi}{\partial y^2}\right)^2\right] \mathrm{d}v + \frac{1}{2}\rho_f g \iint_{B_f} \frac{\partial\Phi}{\partial n}\frac{\partial\Phi}{\partial n}\,\mathrm{d}S, \tag{5}$$

where i is the sub-system index ($i = 1, 2, \ldots$), K is the shell element stiffness matrix, $\mathbf{u}$ the displacement vector of the mean surface of the structure that gives the mode shape, superscript e the element index, N_e the number of the elements in each sub-system and V the fluid domain.

Here the first term gives the elastic energy of the shell structure, the second term gives the potential energy stored by the compressible fluid, and the third term refers to any free surface waves on the fluid.

Similarly, the kinetic energy is given by

$$E_i = \frac{1}{2}\omega^2 \sum_{e=1}^{N_e} \mathbf{u}^{e^{\mathrm{T}}} M^e \mathbf{u}^e + \frac{1}{2}\rho_f \omega^2 \iiint_V \nabla\Phi\cdot\nabla\Phi\,\mathrm{d}v. \tag{6}$$

Here the first term refers to the structure and the second to the fluid. By using Green's theorem the kinetic energy can be simplified into

$$E_i = \frac{1}{2}\omega^2 \sum_{e=1}^{N_e} \mathbf{u}^{e^{\mathrm{T}}} M^e \mathbf{u}^e + \frac{1}{2}\omega^2\rho_f \iint_{B_s+B_f} \Phi\frac{\partial\Phi}{\partial n}\,\mathrm{d}S. \tag{7}$$

Application of the free-surface condition leads to

$$\rho_f g \iint_{B_f} \frac{\partial \Phi}{\partial n} \frac{\partial \Phi}{\partial n} \, \mathrm{d}S = \rho_f \omega^2 \iint_{B_f} \frac{\partial \Phi}{\partial n} \, \mathrm{d}S. \tag{8}$$

Therefore, the potential and kinetic energy share the common term relating to free-surface potential energy, and this can for convenience be eliminated.

Accordingly, the kinetic energy becomes

$$E_i = \frac{1}{2} \omega^2 \sum_{e=1}^{N_e} \mathbf{u}^{e\mathrm{T}} M^e \mathbf{u}^e + \frac{1}{2} \rho_f \omega^2 \iint_{B_s} \Phi \mathbf{u} \cdot \mathbf{n} \, \mathrm{d}S \tag{9}$$

after using the boundary condition B_s.

An alternative for evaluating the energies is achievable by using elemental summation only, without using boundary integration. Both solid and fluid kinetic energies are given by the following equation when appropriate parameters are used.

$$E_i = \frac{1}{2} \omega^2 \sum_{e=1}^{N_e} \{\mathbf{u}^e\}^{\mathrm{T}} [M^e] \{\mathbf{u}^e\}. \tag{10}$$

This formula is more straightforward. However, it becomes less practical when a large number of fluid elements is involved, producing large data files containing elemental mass and stiffness matrices. Limitations also arise when elemental mass/stiffness output is not available for the fluid elements, as in the version of ABAQUS used here. The fluid energy must then be evaluated by using an analogy between fluids and solids: a fluid element can be degenerated from a solid element by restricting its d.o.f.s at the nodes and by specifying its material properties so that the shear modulus vanishes. Equivalent solid elements then have to be used to replace the fluid elements for this purpose. However, an analogous relationship can be established between the fluid potential and solid displacement.

The fluid equation (3) can be written as

$$\frac{\partial}{\partial x}\left(\frac{\partial \Psi}{\partial x}\right) + \frac{\partial}{\partial y}\left(\frac{\partial \Psi}{\partial y}\right) + \frac{\partial}{\partial z}\left(\frac{\partial \Psi}{\partial z}\right) = \frac{1}{c^2} \frac{\partial^2 \Psi}{\partial t^2} \tag{11}$$

and the equation of motion in the solid in, say, the x direction is

$$\frac{\partial \sigma_{xx}}{\partial x} + \frac{\partial \tau_{xy}}{\partial y} + \frac{\partial \tau_{xz}}{\partial z} = \rho \frac{\partial^2 u_x}{\partial t^2}. \tag{12}$$

The above two equations illustrate the analogy if it is assumed that $u_x = \Psi$ and $\rho = 1/c^2$. Thus $\sigma_{xx} = \partial \Psi / \partial x = v_x$, $\tau_{xy} = \partial \Psi / \partial y = v_y$, and $\tau_{xz} = \partial \Psi / \partial z = v_z$. The material properties can be set up accordingly, with equivalent density $\rho = 1/c^2$, where $c^2 = K/\rho_f$, K being the bulk modulus and the stiffness constants E_{11}, E_{44}, E_{55} being equal to 1; or the density $\rho = 1/E$, and the stiffness constants E_{11}, E_{44}, E_{55} being $1/\rho_f$.

Another alternative is to use modal parameters. The response is decomposed by using a set of normalized modes for the sub-systems, associated with appropriate boundary conditions. The response $\{u\}$ is then expressed as

$$\{u_i\} = [\Phi] \{p_i\}. \tag{13}$$

By dividing the modes into categories, for instance, axial, torsional, and bending Φ_a, Φ_t, Φ_b, one can write this as

$$\{x_i\} = [\Phi_a]\{p_a\} + [\Phi_t]\{p_t\} + [\Phi_b]\{p_b\}, \tag{14}$$

where $\{p_a\}$, $\{p_t\}$ and $\{p_b\}$ are principal co-ordinates indicating the contribution to the responses in each mode.

The principal co-ordinates can be determined from

$$\begin{Bmatrix} p_a \\ p_t \\ p_b \end{Bmatrix} = \begin{bmatrix} \Phi_a^{\mathrm{T}}\Phi_a & & \text{sym} \\ \Phi_t^{\mathrm{T}}\Phi_a & \Phi_t^{\mathrm{T}}\Phi_t & \\ \Phi_b^{\mathrm{T}}\Phi_a & \Phi_b^{\mathrm{T}}\Phi_t & \Phi_b^{\mathrm{T}}\Phi_b \end{bmatrix} \begin{bmatrix} \Phi_a^{\mathrm{T}} \\ \Phi_t^{\mathrm{T}} \\ \Phi_b^{\mathrm{T}} \end{bmatrix} \{u_i\}. \tag{15}$$

The elemental summation giving the kinetic energy can then be recast as a modal summation

$$E_i = \frac{1}{2}\omega^2 \sum_{j=1}^{m} M_j p_j^2, \tag{16}$$

where the M_j are modal masses and m is the number of modes used in the expansion (including both solid and fluid modes). This approach has some advantages over the others given above, in terms of ease of manipulation. The method also allows for rapid extraction of the energy levels and only a subset of nodes is required for dynamic response output in the SEA analysis, avoiding the need to create large disk files. It is not necessary to retain element matrices, thus yielding efficiency in evaluating sub-system energies. In addition, the modal contribution factors can be used as building blocks for creating modal sub-systems.

A number of tests were performed using these various approaches and good agreement found between them up to 1000 Hz, provided that in the modal calculations some 40 modes were used for each straight section in the system and 20 modes for the bend. Some liquid resonances were observed, but the equivalent energy levels were small in comparison to those of the shell resonances.

3.2. POWER INJECTION ANALYSIS

In general an SEA model consists of many interconnected sub-systems, with each sub-system being connected to some or all of the others and with some or all being subject to external loading. This model varies depending on how the overall system is split into sub-systems and how the sub-systems are topologically interlinked.

Consider a system of n interconnected sub-systems for which $\pi_{i,in}$ is the power injected into sub-system i, $\pi_{i,d}$ is the power lost due to dissipation in sub-system i, π_{ij} is the net energy flowing from system i to system j. A simple power balance analysis for each of the sub-systems gives rise to a system of linear equations relating input powers and sub-system energies to the loss and coupling loss factors η_{ij}: i.e.,

$$\{P\} = [X]\{E\}, \tag{17}$$

where the loss factor matrix $[X]$ is defined as

$$[X] = \begin{bmatrix} \eta_{1,t} & -\eta_{21} & -\eta_{31} & \cdots & -\eta_{n1} \\ -\eta_{12} & -\eta_{2,t} & -\eta_{32} & \cdots & -\eta_{n2} \\ -\eta_{13} & -\eta_{23} & -\eta_{3,t} & \cdots & -\eta_{n3} \\ \vdots & \vdots & \vdots & \ddots & \vdots \\ -\eta_{1n} & \eta_{2n} & -\eta_{3n} & \cdots & -\eta_{n,t} \end{bmatrix}, \tag{18}$$

with

$$\eta_{i,t} = \sum_{j=1}^{n} \eta_{ij}. \tag{19}$$

$\{P\}$ is given by

$$\{P\} = \begin{Bmatrix} \pi_{1,in} \\ \pi_{2,in} \\ \vdots \\ \pi_{n,in} \end{Bmatrix} \tag{20}$$

and $\{E\}$ is a column vector of the energies of each of the sub-systems. η_{ii} is the loss factor of the ith sub-system (i.e., that due to internal damping) and $\eta_{ij}(i \neq j)$ is the coupling loss factor controlling energy flow from sub-system i to j.

The energy level of each sub-system is thus estimated by

$$\{E\} = [X]^{-1}\{P\}. \tag{21}$$

If all the entries of $[X]$ consisting of loss factors and coupling loss factors are known, the energy of each sub-system can be determined from equation (21) for a given input power vector $\{P\}$, and in turn the space- and time-averaged velocity or pressure in the sub-systems may be determined.

When the coupling loss factors and loss factors are unknown, they can be found by computing the energy of each sub-system for a known input power, from the average velocity or pressure. This is the principle of the power injection method used here. To extract the loss factors and coupling loss factors, each sub-system is excited, one at a time, thereby generating an independent set of linear equations ($n \times n$ or more) relating the energy of the n sub-systems to the input power corresponding to the n or more sets of simulations or measurements.

Accordingly, equation (17) may be set in a matrix form as

$$[P] = [X][E], \tag{22}$$

where $[P]$ and $[E]$ are obtained by collating power and energy vectors with respect to all the required loadings, $[P] = [\{P_1\}, \{P_2\}, \ldots, \{P_n\}]$, $[E] = [\{E_1\}, \{E_2\}, \ldots, \{E_n\}]$, in which, $\{P_i\}$ and $\{E_i\}$ each contain details for all sub-systems for load case i.

Commonly, more test cases are used than necessary to create more equations than unknowns and then a least-squares fit is used to extract $[X]$ whose entries consist of loss and coupling loss factors (and zeros are imposed where there are no direct energy paths between sub-systems). This does, unfortunately, mean that if a loading case identical to one of the test cases is studied using the resulting SEA model it will not, in general recover the

original results with perfect fidelity. Rather, the aim is to give good, as opposed to perfect results, across a spread of loading cases.

In general, one may transpose equation (22), to obtain

$$[P]^{\mathrm{T}} = [E]^{\mathrm{T}}[X]^{\mathrm{T}}, \tag{24}$$

with

$$[X]^{\mathrm{T}} = [\{\eta_1\}, \{\eta_2\}, \{\eta_3\}, \ldots, \{\eta_n\}], \qquad [P]^{\mathrm{T}} = [\{P_1 T\}, \{P_2 T\}, \ldots, \{P_n T\}], \tag{25, 26}$$

and

$$[E]^{\mathrm{T}} = [\{E_1 T\}, \{E_2 T\}, \ldots, \{E_n T\}], \tag{27}$$

where

$$\{P_j T\} = \{P_{1j}, P_{2j}, \ldots, P_{nj}\}^{\mathrm{T}}, \qquad \{E_j T\} = \{E_{1j}, E_{2j}, \ldots, E_{nj}\}^{\mathrm{T}},$$

for each sub-system j and experiments 1 to n. It should be noted that not all elements in $[X]$ are independent because of the zeros being prescribed by the non-linkage between some sub-systems.

By expanding $[X]$ the loss factors may be rearranged in vector form as

$$\{\eta\} = \begin{Bmatrix} \{\eta_1\} \\ \{\eta_2\} \\ \vdots \\ \{\eta_n\} \end{Bmatrix}, \tag{28}$$

where $\{\eta_i\} = \{\eta_1^i, \eta_2^i, \ldots, \eta_n^i\}^{\mathrm{T}}$. Therefore, the following augmented equation may be derived:

$$\begin{bmatrix} E^{\mathrm{T}} & 0 & \ldots & 0 \\ 0 & E^{\mathrm{T}} & \ldots & 0 \\ \vdots & \vdots & \ddots & \vdots \\ 0 & \ldots & 0 & E^{\mathrm{T}} \end{bmatrix} \begin{Bmatrix} \{\eta_1\} \\ \{\eta_2\} \\ \vdots \\ \{\eta_n\} \end{Bmatrix} = \begin{Bmatrix} \{P_1 T\} \\ \{P_2 T\} \\ \vdots \\ \{P_n T\} \end{Bmatrix}. \tag{29}$$

This may be written as

$$[\bar{E}]\{\eta\} = \{\bar{P}\}, \tag{30}$$

where $[\bar{E}]$ has an many rows as experiments times sub-systems, and columns as sub-systems squared, etc. As has been noted, the number of equations usually exceeds the number of variables; hence the need to use a least-square fit. The non-zero independent entries in $\{\eta\}$ are then compressed as $\{\zeta\}$ and a link table constructed whose entries are either unity or zero (indicating the presence or absence of direct interconnections).

A Bole's matrix $[B]$ can then be derived from a unit matrix by removing those columns (unit vectors) where the corresponding linkage does not exist. Consequently,

$$\{\eta\} = [B][\zeta]. \tag{31}$$

The number of variables is thus reduced to the number of independent variables obtainable by adding up the binaries in the link table. The normal equation corresponding to equation

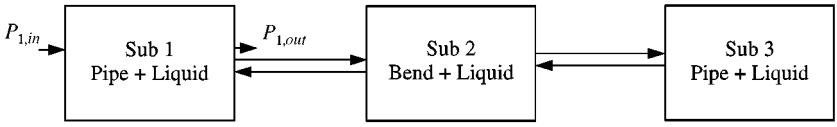

Figure 4. Series modal for the three section pipe-work problem.

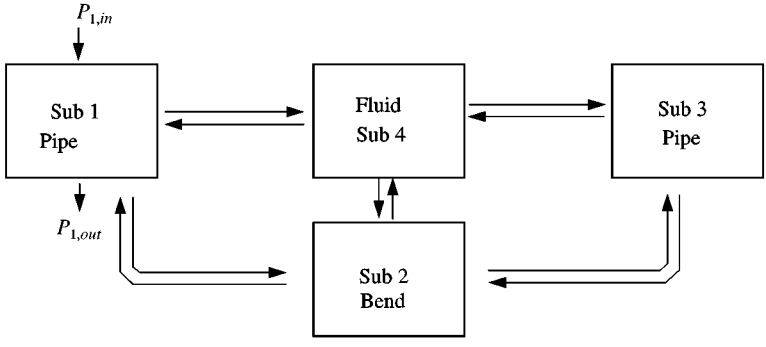

Figure 5. Four sub-system model based on three structures plus the fluid.

(30) is then obtained as

$$[B]^{\mathrm{T}}[\bar{E}]^{\mathrm{T}}[\bar{E}][B]\{\zeta\} = [B]^{\mathrm{T}}[\bar{E}]^{\mathrm{T}}\{\bar{P}\}. \tag{32}$$

By solving this system of linear equations, $\{\zeta\}$ is obtained and $[X]$ can be recovered and then used with further input powers to deduce energy levels for new situations.

3.3. SEA MODELS

Given the nature of pipework systems, the most basic SEA model that can be considered is where each piece of pipe is modelled as a single sub-system with series connections between them. For such series models, energy flow only takes place between adjacent sub-systems. The linkage table is then a tridiagonal matrix. Applied to the three-part FE model used here, each part is taken as a sub-system which consists of both liquid and shell (see Figure 4).

According to Brevart and Fuller [16], and perhaps not surprisingly, energy exchange occurs between the liquid and the shells suggesting that energy flows not only between the shell sections but also between the shell and the liquid. Consequently, a more complex parallel model was considered next, in which the three shells and the liquid are taken as separate sub-systems (i.e., four sub-systems in total) (see Figure 5).

The final level of the SEA model considered here is based on the varying classes of vibrational modes that occur in the dry shells. It is often stated in SEA modelling that different classes of mode types should not be mixed within a single sub-system and so here a model has been built where three types of modes are used: i.e., axial, torsional, and bending modes. The sub-systems are then created by grouping the modal contribution factors obtained through modal decomposition according to mode type. The sub-system energies can then be evaluated by following equation (16) and summing over the

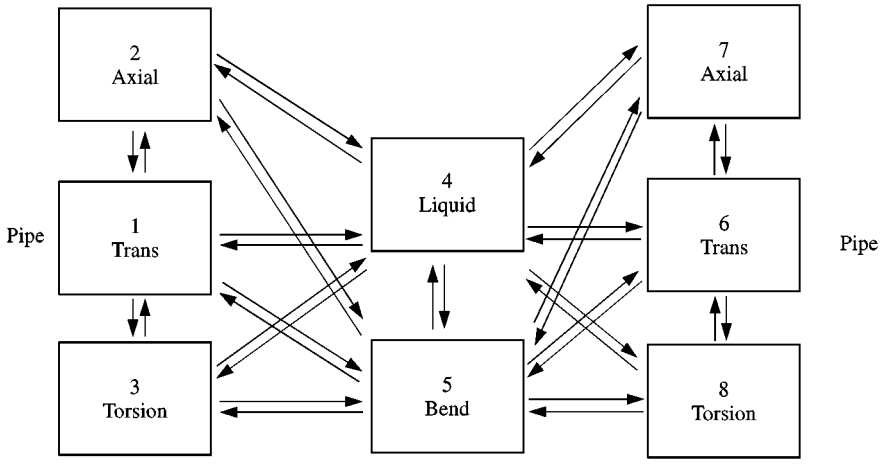

Figure 6. Eight sub-system model in which mode types are the basis of the sub-systems.

appropriate set of modes. Figure 6 illustrates this modal interaction model. Here, 40 dry modes have been used for each straight section of pipe, of which 17 are bending, 11 axial and 12 torsional, spanning the frequency range from 0 to 1000 Hz. Given that the modes do not separate into different classes for the bend this sub-system consists of all its dry modes. Finally, the liquid throughout the whole pipe run constitutes an additional eighth sub-system. Note also that the liquid and pipe-bend possess fewer modes than the straight sections which provides a further justification for not breaking down their modes to form multiple sub-systems.

3.4. TEST CASES—NO AVERAGING

After having set out the analysis methods to be used and the three SEA models to be studied, attention is next turned to a series of numerical experiments which act as test cases. The main purposes of these tests is to ascertain which kind of SEA model gives the most reliable results, and also to see how well simple models perform, since in many cases they may prove adequate for preliminary design work and would certainly be easier to use in practice.

In each case, the loss and coupling loss factors of the SEA models are derived from a series of 10 single-point loading calculations using the FE methods outlined above and averaged together by the least-squares matrix solution methods also described above. These results are all for unit power input (obtained from unit forcing by dividing by the actual energy inputs). Moreover, for each model studied the same forcing sets have been used in deriving the SEA coefficients so that the same input information is used in each case. Results are first presented without being averaged or integrated over frequency to gain frequency by frequency understanding of the models. Results are then presented for frequency band averaged data.

The forces used to load the first straight section of pipe were as follows: (1) two axial forces acting along the pipe applied symmetrically to a pair of midspan nodes; (2) a pair of equal and opposite forces applied transversely to a pair of midspan nodes at either end of a common diameter; (3) a single transverse point load applied at midspan. For the pipe-bend the forces were (4) a pair of forces applied at 45° to the surface, in line with the first section, half-way around the bend at either end of a common diameter and in the same

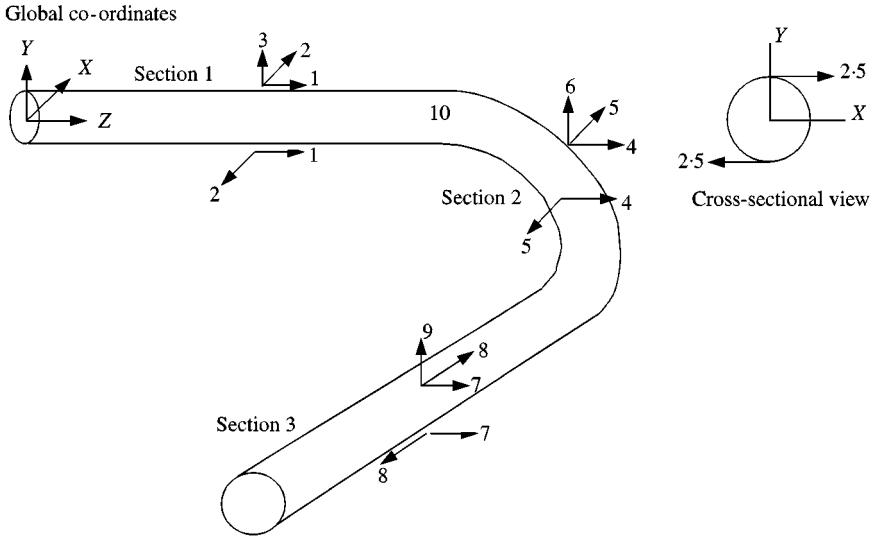

Figure 7. Forces used in the test cases.

direction; (5) a pair of equal and opposite forces applied transversely to a pair of mid-bend nodes at either end of a common diameter and normal to the pipe, and (6) a single transverse force applied at mid-bend, normal to the pipe and also the plane of the bend. The second straight section was forced with (7) a pair of transverse forces applied at midspan at either end of a common diameter and at right angles to the pipe; (8) a pair of equal and opposite forces applied in line with the pipe at a pair of midspan nodes at either end of a common diameter, and (9) a single transverse force applied at a midspan node at right angles to the plane of the bend. The internal liquid was also excited by a direct variation in the internal pressure (10). This array of forces was designed to provide a range of types of excitation that would cause significant motions across all mode types. They are illustrated in Figure 7.

Figures 8–10 show the middle frequency results for the first SEA model with just three sub-systems, giving energy levels for sub-systems 1–3 respectively. In each figure, the curves show the energy levels predicted when sub-systems 1 and 3 are forced at the same time, with sub-system 1 loaded axially at midspan by two point forces and sub-system 3 transversely, also at midspan and by two point forces. The solid lines in the figures show the energies predicted by the FE approach and these are compared to two SEA estimates in each case.

The first of the SEA estimates is based on coupling loss factors deduced from the full series of 10 experiments where forces have been applied to each of the three sub-systems in turn while at the same time enforcing the requirement that energy flow only where the SEA model being used has direct connections: i.e., some of the elements of $[X]$ are zero. This is here termed the "full" SEA model and would be the approach that most users of SEA would say reflects normal practice for unaveraged work.

The second SEA estimate allows energy to flow between all sub-systems, irrespective of whether they are directly connected or not (allowing tunnelling or indirect coupling) and, additionally, is based on a reduced set of three force cases that are similar to those of the direct FE calculation used in the test case: here termed the "ideal" SEA model. This estimate is designed to show the best agreement that can reasonably be expected in this type of analysis and allows the relative errors in the "full" SEA model to be more readily interpreted.

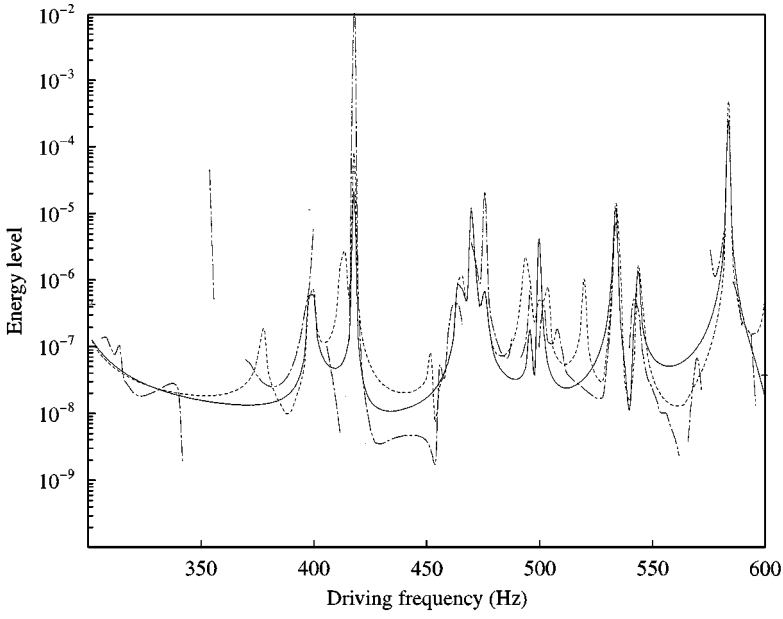

Figure 8. Comparison of the energies from the direct FE simulations and by predictions using SEA model 1 for sub-system 1, first straight pipe and liquid: ——, FE; - - - -, "ideal" SEA - — - —, "Full" SEA; crosses mark individual positive points in the full SEA curve.

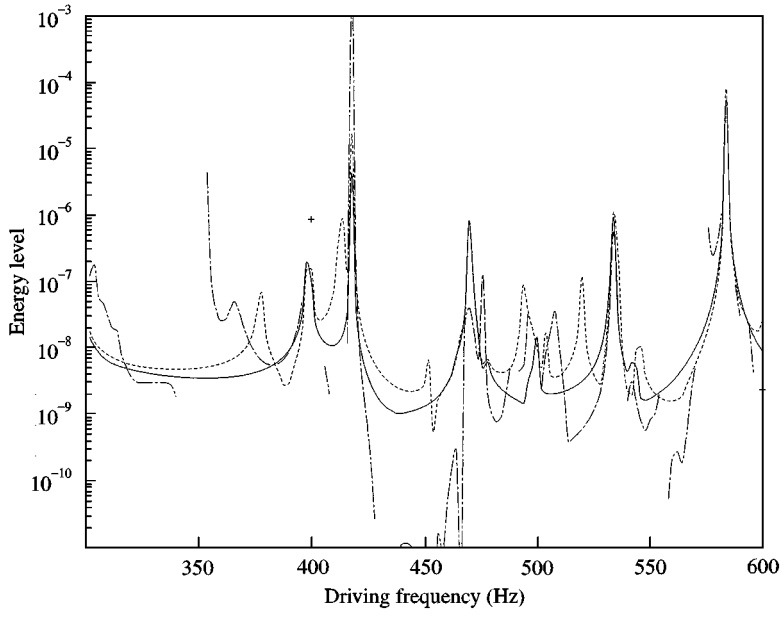

Figure 9. Comparison of the energies from the direct FE simulations and by predictions using SEA model 1 for sub-system 2, pipe bend and liquid: ——, FE; - - - -, "ideal" SEA - — - —, "Full" SEA.

As can be seen from the figures the three curves agree reasonably well most of the time, particularly near the resonances of the system. However, at certain frequencies the "full" SEA model predicts negative energy levels (where the curve is missing from the figures since

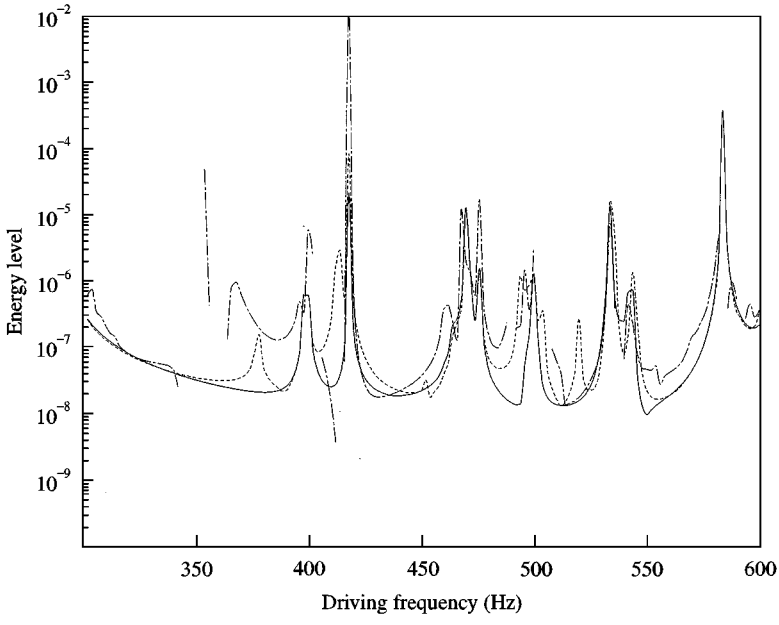

Figure 10. Comparison of the energies from the energies from the direct FE simulations and by predictions using SEA model 1 for sub-system 3, second straight pipe and liquid: ——, FE; - - - -, "ideal" SEA - — - —, "Full" SEA.

they are plotted on log scales). At these points the coefficients in the SEA model do not have their normal physical significance in that they indicate for example, energy flowing towards the source of forcing and not away (i.e., uphill). This is a consequence of imposing too many requirements on the modelling with insufficient data to support it.

Note also that the "full" SEA models show some resonances that are not present in practice because the forcing model used for the test case does not excite all the modes of the system, while the data used to prepare the coefficients in the models are based on forcing that does. It is also clear that the bend sub-system (sub-system 2) has a lower overall energy level (it has, after all, lower mass) and this is clearly much harder to predict with accuracy.

The "ideal" SEA model performs well throughout the range of frequencies and has no negative energy levels because energy flows are permitted directly between all three sub-systems: i.e., less constraints are imposed on the sub-systems but at the expense of allowing coupling losses to occur between systems that are not directly connected. Even allowing for this they form a rather unrealistic set of curves because one really needs to know the answers before asking the questions to adopt this kind of approach, or, at the very least, to build the SEA model using forcing loads that are extremely close in nature to those for which subsequent estimates are to be obtained. Note also that although the "ideal" model gives better results this does not mean that the relevant coupling loss and loss factors are all positive, rather the elements of the $[X]$ matrix are just well suited to predicting the sub-system energy levels. They are sometimes negative and/or have extremely large magnitudes.

Figures 11–14 show the same data as Figures 8–10 for the same loading case, but now for the four sub-system model where the liquid is treated as a separate sub-system. Here, the bend sub-system is modelled slightly less well (it has even less mass) but the liquid predictions (sub-system 4) are in quite good agreement. The agreement for the straight pipe

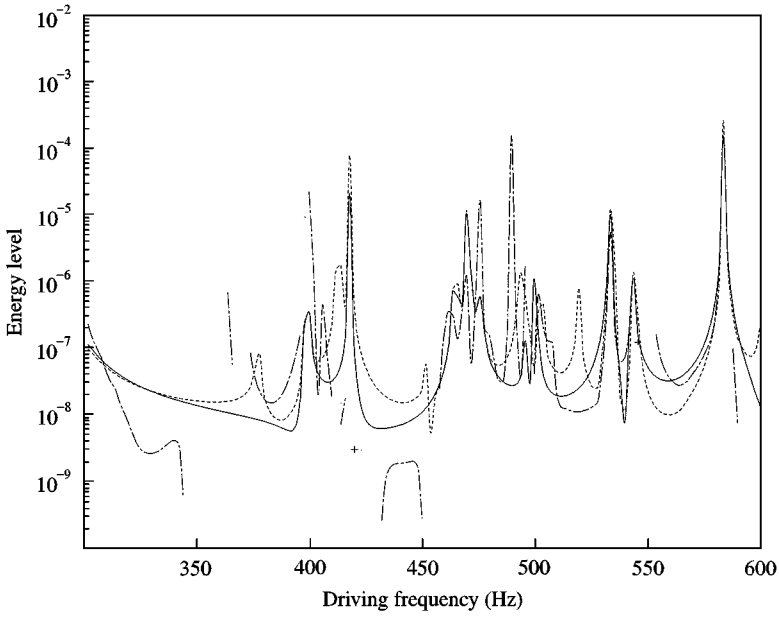

Figure 11. Comparison of the energies from the direct FE simulations and by predictions using SEA model 2 for sub-system 1, first straight pipe: ——, FE; - - - -, "ideal" SEA - — - —, "Full" SEA.

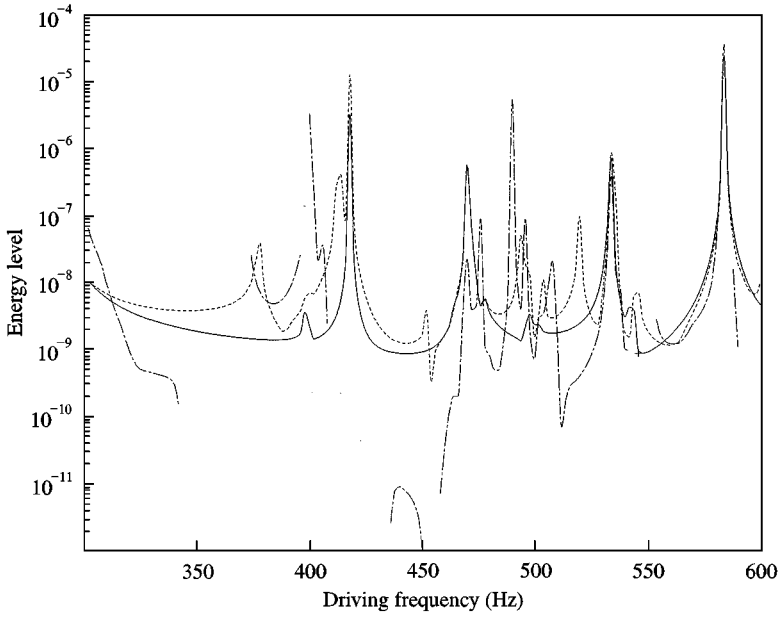

Figure 12. Comparison of the energies from the direct FE simulations and by predictions using SEA model 2 for sub-system 2, pipe bend: ——, FE; - - - -, "ideal" SEA - — - —, "Full" SEA.

sections is also slightly improved. Overall, however, the differences are slight and there seems to be little gained from separating out the liquid system in this way unless information is specifically required on the energy levels of the liquid.

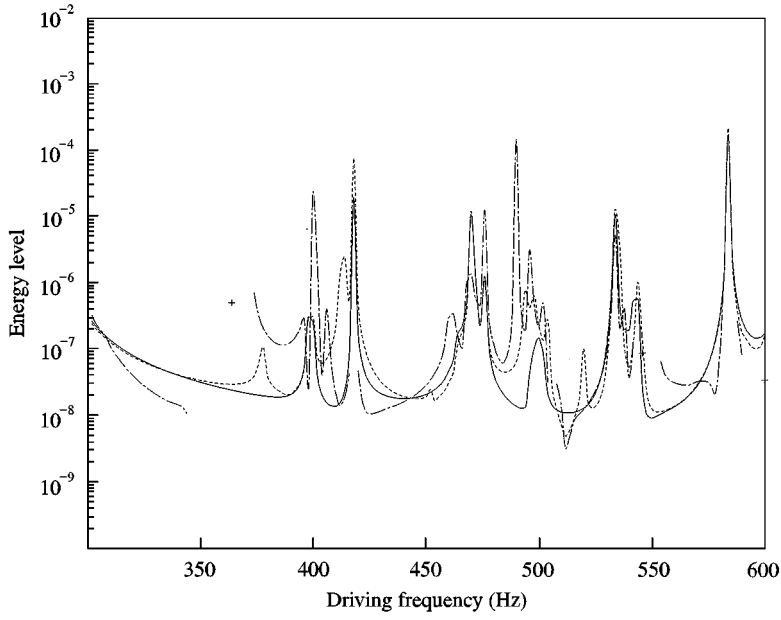

Figure 13. Comparison of the energies from the direct FE simulations and by predictions using SEA model 2 for sub-system 3, second straight pipe: ——, FE; - - - -, "ideal" SEA - — - —, "Full" SEA.

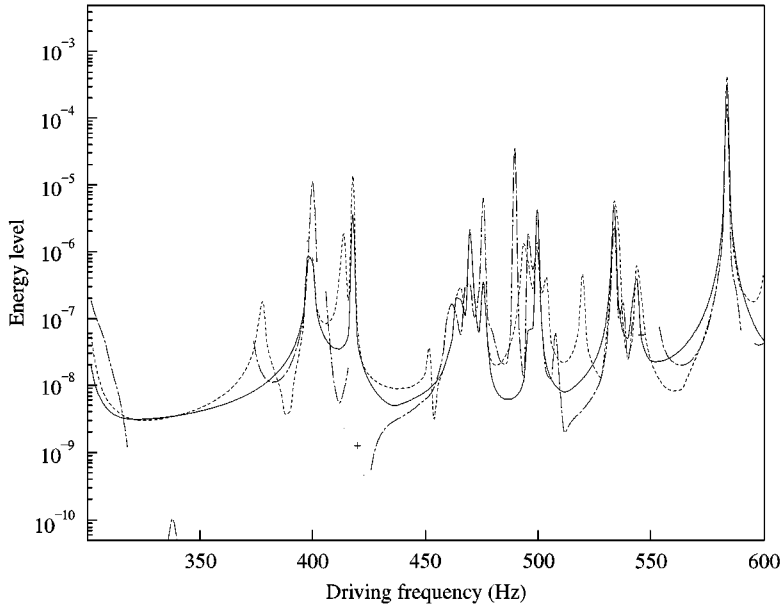

Figure 14. Comparison of the energies from the direct FE simulations and by predictions using SEA model 2 for sub-system 4, liquid: ——, FE; - - - -, "ideal" SEA - — - —, "Full" SEA.

Figures 15–22 again show the same data as Figures 8–10 for the same loading case, but in this case for the eight sub-system model where the straight section mode groups and the liquid are treated as individual sub-systems. This is the most complex SEA model considered here and it might be expected to yield the best results. In this case, the "ideal"

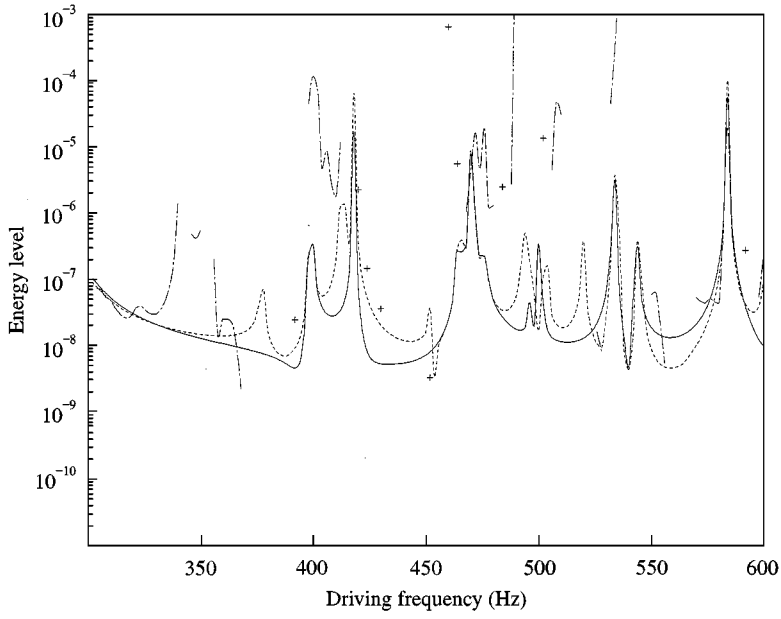

Figure 15. Comparison of the energies from the direct FE simulations and by predictions using SEA model 3 for sub-system 1, transverse modes, first straight pipe: ——, FE; - - - -, "ideal" SEA - — - —, "Full" SEA.

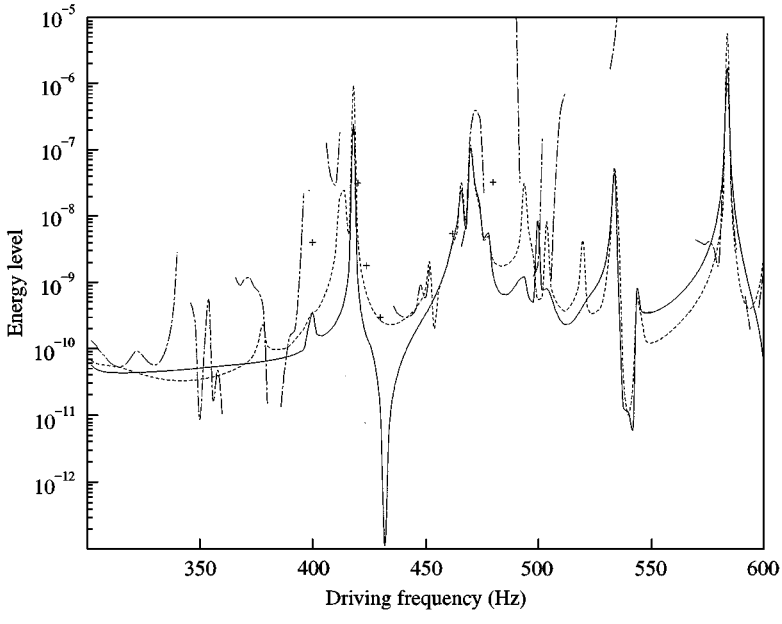

Figure 16. Comparison of the energies from the direct FE simulations and by predictions using SEA model 3 for sub-system 2, axial modes, first straight pipe: ——, FE; - - - -, "ideal" SEA - — - —, "Full" SEA.

model again gives quite good results throughout, although there are some discrepancies for sub-systems 7 and 8 which are at rather low energy levels. This is by no means the case for the "full" model, however: while the bending mode sub-system of the first pipe is quite well predicted, the axial mode predictions give negative results for many frequencies and the

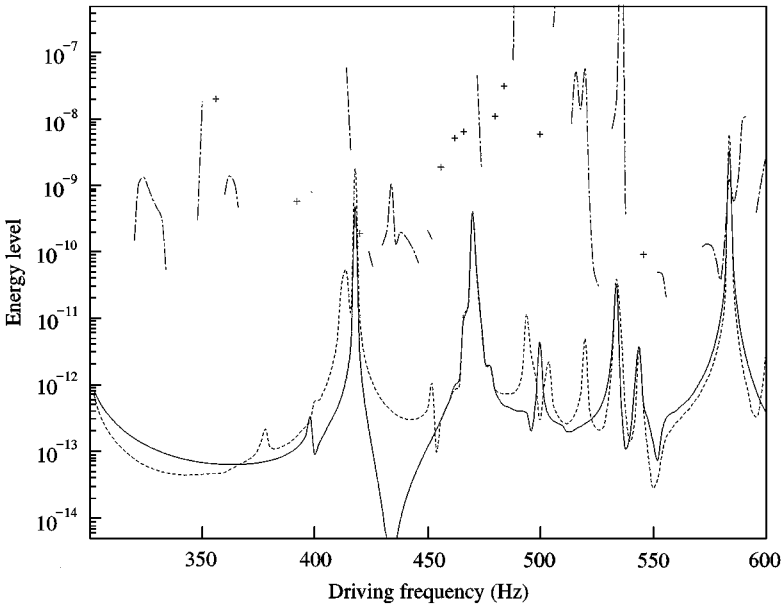

Figure 17. Comparison of the energies from the direct FE simulations and by predictions using SEA model 3 for sub-system 3, torsional modes, first straight pipe: ——, FE; - - - -, "ideal" SEA - — - —, "Full" SEA.

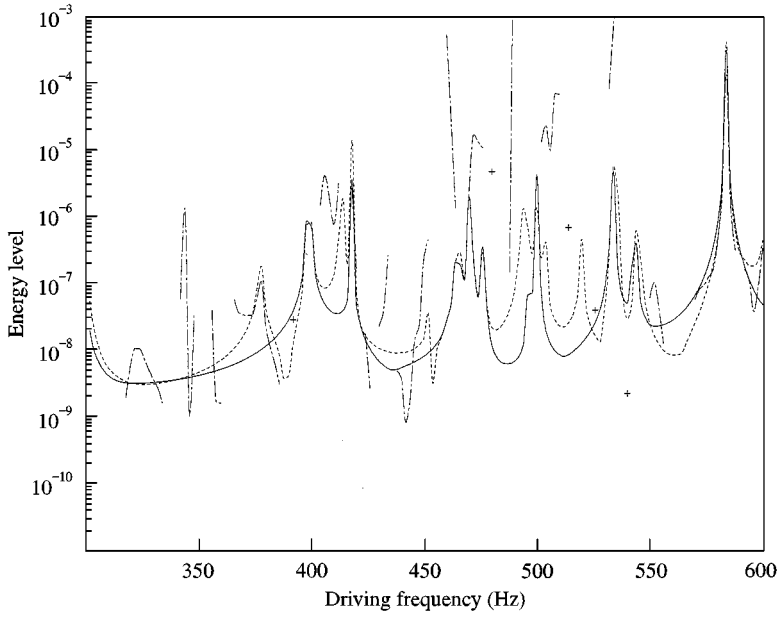

Figure 18. Comparison of the energies from the direct FE simulations and by predictions using SEA model 3 for sub-system 4, liquid: ——, FE; - - - -, "ideal" SEA - — - —, "Full" SEA.

torsional mode results are typically two orders of magnitude in error (although this is at very low energy levels). For this model the liquid sub-system (sub-system 4) is quite well predicted but his is not so accurate as in model 2 (cf., Figure 14) while the pipe-bend is probably slightly better predicted than in model 2 (cf., Figure 12). The results for the other

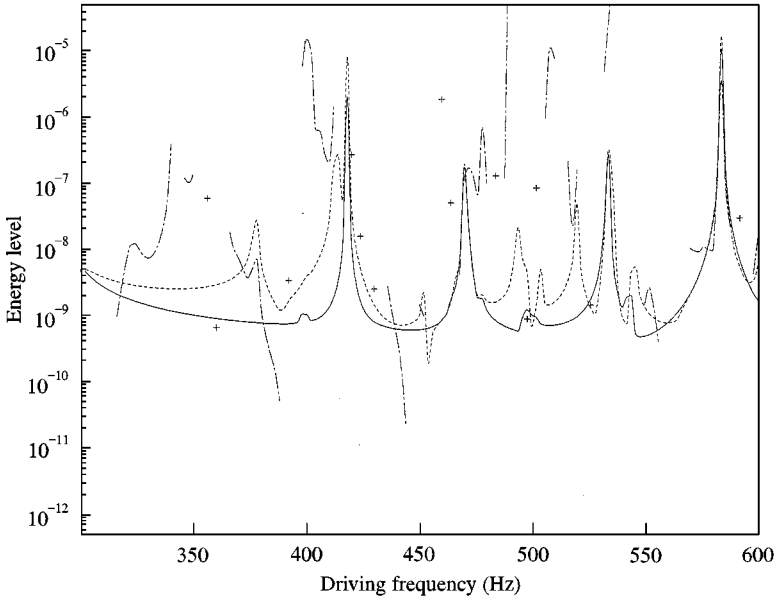

Figure 19. Comparison of the energies from the direct FE simulations and by predictions using SEA model 3 for sub-system 5, pipe bend: ——, FE; - - - -, "ideal" SEA - — - —, "Full" SEA.

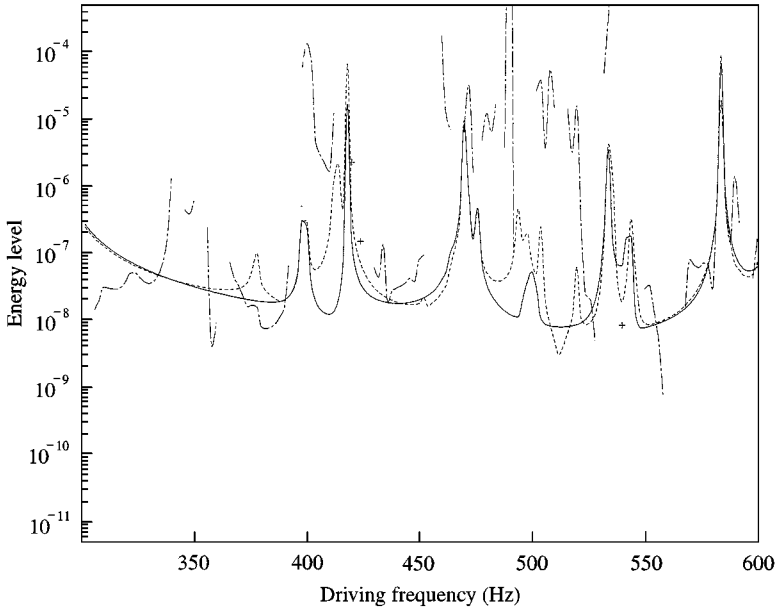

Figure 20. Comparison of the energies from the direct FE simulations and by predictions using SEA model 3 for sub-system 6, transverse modes, second straight pipe: ——, FE; - - - -, "ideal" SEA - — - —, "Full" SEA.

straight section are again not very pleasing with the torsional modes again badly predicted although the bending modes are quite well modelled.

It is not immediately obvious why these results are worse than the previous, simpler models but it seems that the lack of large numbers of individual modes within the

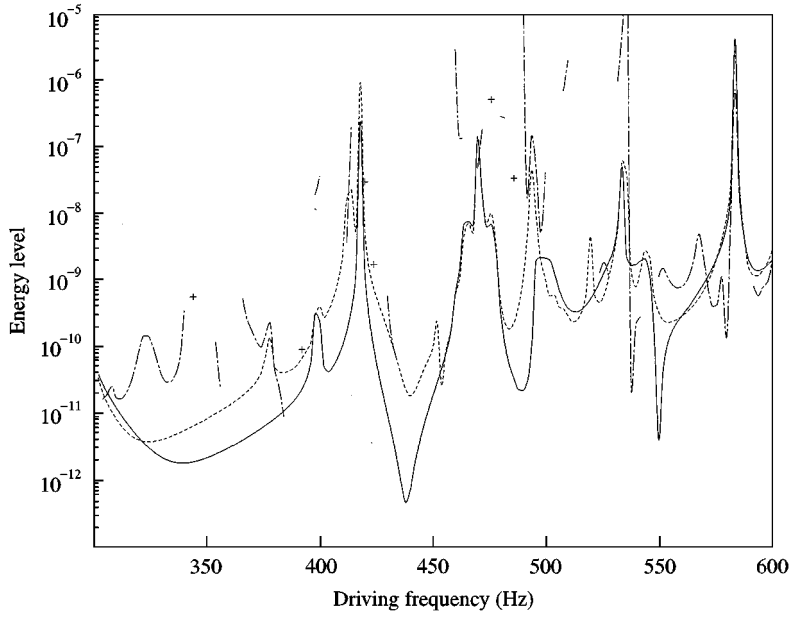

Figure 21. Comparison of the energies from the direct FE simulations and by predictions using SEA model 3 for sub-system 7, axial modes, second straight pipe: ——, FE; - - - -, "ideal" SEA - — - —, "Full" SEA.

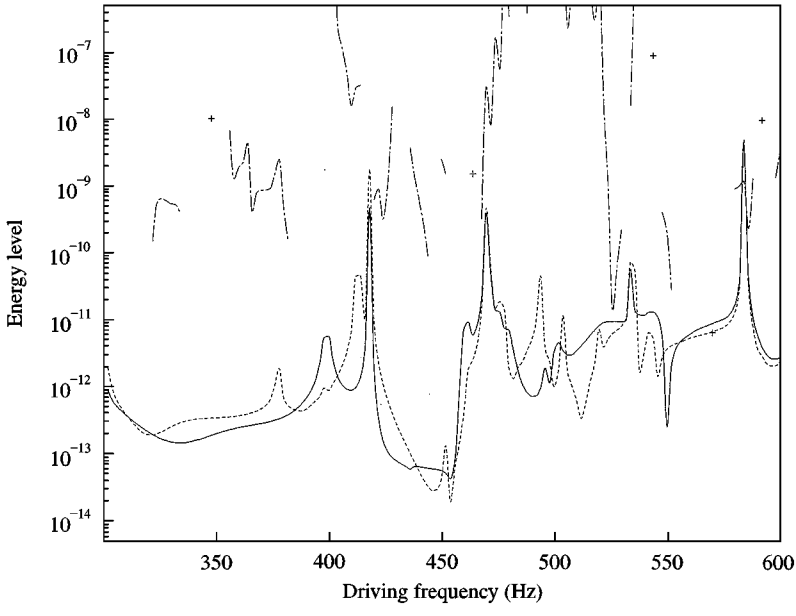

Figure 22. Comparison of the energies from the direct FE simulations and by predictions using SEA model 3 for sub-system 8, torsional modes, second straight pipe: ——, FE; - - - -, "ideal" SEA - — - —, "Full" SEA.

sub-systems must be one cause. Although no sub-system in this model contains less than 10 modes, over the range of frequencies studied here rather less than half of these are actually excited. It would also appear to be the case that enforcing more and more complex topological requirements on the energy flow paths by adopting more involved models tends

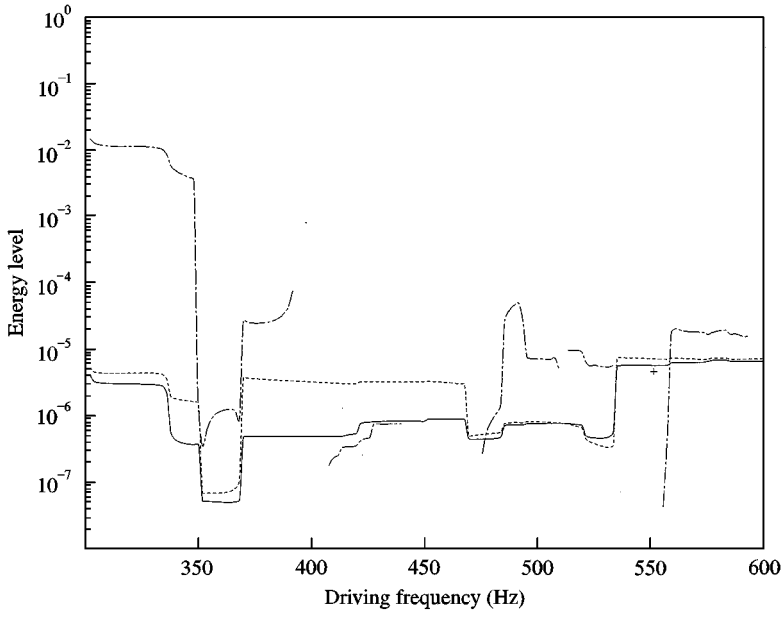

Figure 23. Comparison of the energies from the direct FE simulations and by predictions using SEA model 1 for sub-system 1, first straight pipe and liquid, data averaged over 100 Hz frequency bands: ——, FE; - - - -, "ideal" SEA - — - —, "Full" SEA.

to reduce the numerical stability of the power injection process and this may also contribute to the rather poor performance of the third SEA model. Finally, the ratio of sub-systems to experiments is rather high in this case in that coefficients for eight sub-systems are being derived from the results of just 10 experiments. Using more data would also help average the results but equally might also improve the results for the simpler models.

3.5. TEST CASES—WITH AVERAGING

Next, attention is turned to the technique of data averaging. One of the characteristics of the traditional SEA approach is to average away some of the predictions that would be clearly wrong in the hope that the averaged behaviour is more meaningful—of course, this can mislead the user into thinking that SEA is performing better than it actually is and is why single frequency, deterministic studies have been presented here first. The approach of *frequency* averaging is commonly used in applied SEA, as opposed to the ensemble averaging used in many theoretical derivations for SEA. It is simple to apply and does not require the sets of similar but varying experimental models needed to form ensemble averages, while still allowing resonance details to be smoothed out. Here this is achieved with a simple moving average of 100 Hz width applied to the experimental data before the application of the power injection method. That is, all the equations are applied as before except to data that have been previously averaged.

For the sake of brevity, this approach is applied only to the three sub-system model previously described. Figures 23–25 are thus equivalent to Figures 8–10 in all respects except for the application of the averaging window before other calculations. As can be seen from the figures the ideal model again performs well, especially at higher frequencies. Once again, the full model does less well, with regions where the predicted energy levels are again

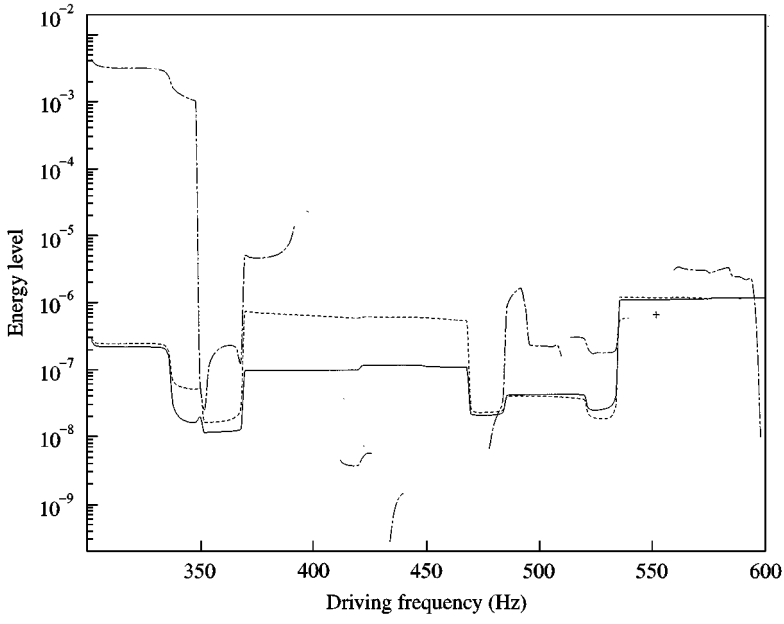

Figure 24. Comparison of the energies from the direct FE simulations and by predictions using SEA model 1 for sub-system 2, pipe bend and liquid, data averaged over 100 Hz frequency bands: ——, FE; - - - -, "ideal" SEA - — - —, "Full" SEA.

negative. Moreover, even when positive, there are frequencies where the results are three orders of magnitude in error. Even so, the results for the three sub-system model remain better than for the other models described earlier when averaged in this way (figures are not presented for these models due to space limitations). Thus, it may be said that frequency averaging does not overcome the basic difficulties of using the power injection method to model this fluid-loaded system unless the experiments used to construct the model are reasonably similar to the forces likely to be seen in practice.

Lastly, attention is turned to the loss and coupling loss factors produced for the frequency-averaged "full' model for this three sub-system configuration. It will be recalled that these can be recovered from the loss factor matrix by using equations (18) and (19). In this case there are three loss factors, one for each sub-system (η_{11}, η_{12} and η_{33}) and four coupling loss factors (η_{12}, η_{21}, η_{23} and η_{32}). These quantities should all be positive and small. The loss factors are plotted in Figure 26 and the coupling loss factors in Figure 27. These plots are rather better behaved than one might expect from the previous three figures since for much of the range of frequency considered they are indeed small and positive. The most notable exception is the bend loss factor η_{22} which is sometimes quite large and also negative for much of the plot. Physically, this implies that energy is being generated in the bend where, of course, none is actually being injected. So even when using 10 sets of experimental data with frequency averaging, good results for the seven factors are not easily recovered.

4. CONCLUSIONS

This paper has described a finite element (FE)-based study of the vibration analysis of a liquid-filled pipe system in the context of statistical energy analysis. FE models for the

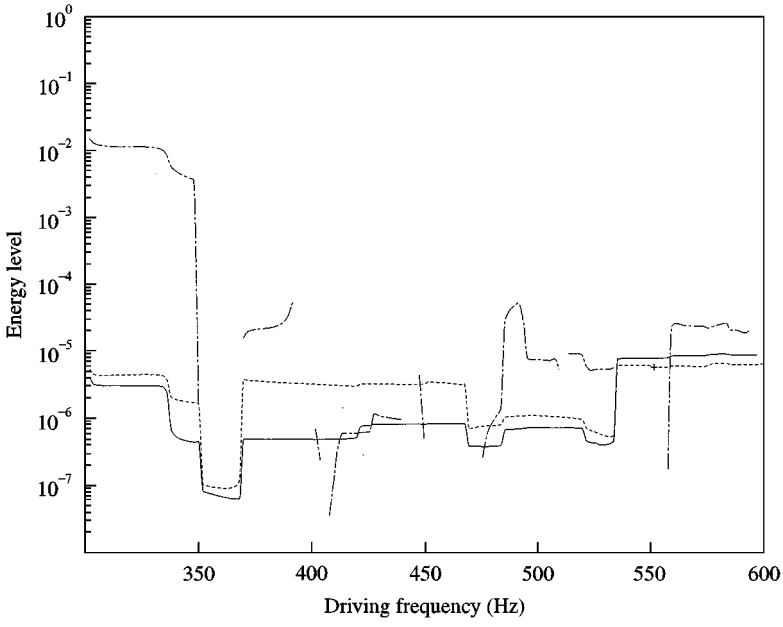

Figure 25. Comparison of the energies from the direct FE simulations and by predictions using SEA model 1 for sub-system 3, second straight pipe and liquid, data averaged over 100 Hz frequency bands: ——, FE; - - - -, "ideal" SEA - — - —, "Full" SEA.

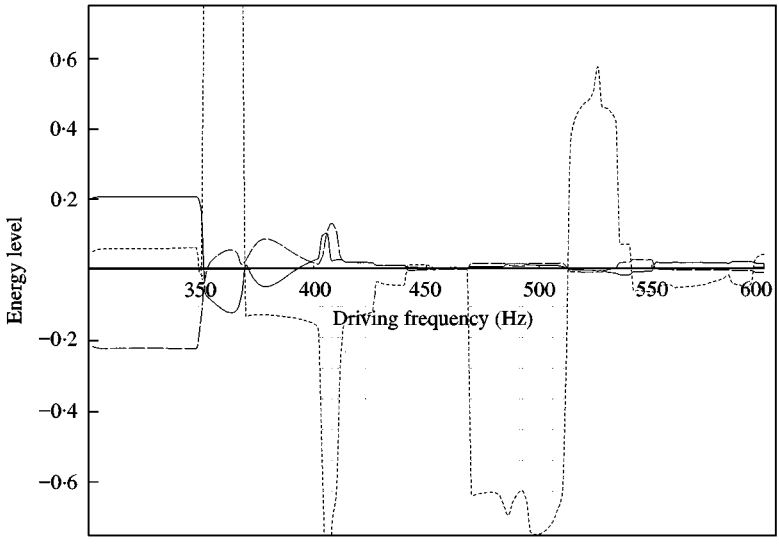

Figure 26. Frequency averaged loss factors for the "full" SEA, three sub-system model: ——, η_{11}; - - - - -, η_{22}; — —, η_{33}.

structure–liquid coupled systems have been set up and the frequency response analysis is undertaken. A direct finite element solution was complemented with a modal representation of the structures and the liquid.

Three SEA models with various interconnections were then devised and used in evaluating the energy flows within the system. These SEA models have been built by

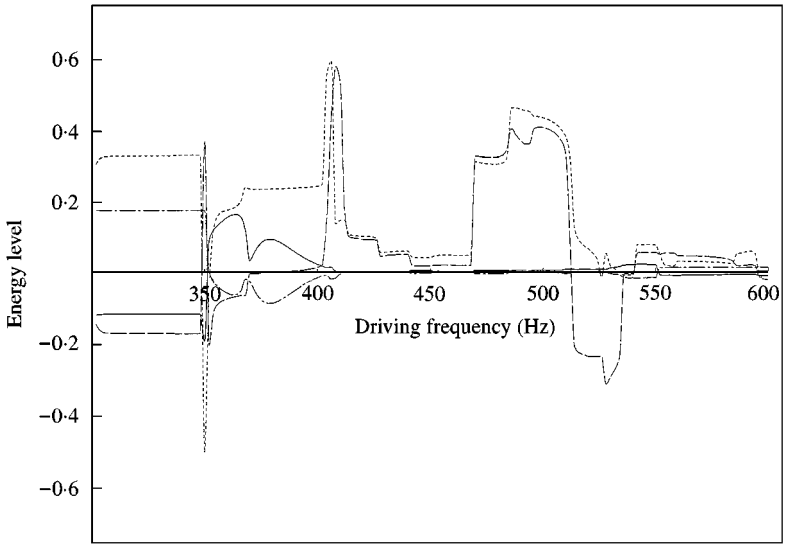

Figure 27. Frequency averaged coupling loss factors for the "full" SEA, three sub-system model: ——, η_{12}; - - - - -, η_{21}; — — — — η_{23}, - — - — - —, η_{32}.

analyzing 10 input data sets and they have then been applied to a combined loading test case where a comparison between the results predicted by the SEA models and direct simulations from the FE analysis has been carried out.

The example studied shows that it is not necessary to adopt modal sub-systems to obtain the most accurate predictions of energies levels for this problem. In fact, a simple linear model of the liquid and structure for each section of pipe being lumped together to form a sub-system gives results that are at least as good as those from a complicated modal decomposition, given the same input data. This appears, at least in part, to be due to the low modal densities that can result when structures are split down to individual mode types and also the more complex topological relationships that must then be enforced in the energy flow matrices. Even so, none of the models considered gives very good results unless the experimental data used is limited to being strongly similar to the loading cases studied subsequently. It is by no means obvious how the shortcomings of more broad ranging SEA models might be improved. Perhaps using additional experimental results might be of benefit. Certainly, breaking the problem down into more sub-systems without adding such additional data does not appear to help. Frequency averaging seems to be of limited use in such circumstances.

These conclusions suggest that it may be possible to build a library of liquid-filled pipe elements that could be used to approximate the energy flows around pipework systems with reasonable accuracy, provided that they were constructed by using loading information similar to that to be studied subsequently. Moreover, such models might be constructed without recourse to the detailed FE models used here if a number of simplifying assumptions are made, such as those adopted by Finnveden [17]. The construction of more general SEA models, especially those involving bends, would seem to be still rather problematical. It also remains the case, of course, that if a long pipework run is being analyzed any errors occurring in predicting energy transmission will be cumulative along the system, even if individual transfers are reasonably well predicted, a feature of such topologies that has been noted before [18].

ACKNOWLEDGMENT

This research was supported by EPSRC grant GR/K82178 as part of the Marine Technology Directorates's Managed Programme on Statistical Energy Analysis.

REFERENCES

1. N. M. PRICE, A. J. KEANE, R. EATOCK TAYLOR and M. LIU 1998 *Journal of Sound and Vibration*, **218**, 361–387. Vibrations of cylindrical pipes and open shell.
2. F. J. FAHY 1996 *Statistical Energy Analysis*. (A. J. Keane and W. G. Price, editors), 1–18. Cambridge: Cambridge University Press. Statistical energy analysis, a critical overview.
3. A. W. LEISSA 1973 *NASA-SP*-288. Vibrations of shells.
4. C. R. CALLADINE 1983 *Theory of Shell Structures*. Cambridge: Cambridge University Press.
5. W. FLÜGGE 1962 *Stresses in Shells*. New York: Springer-Verlag.
6. S. FINNVEDEN 1997 *Journal of Sound and Vibration* **208**, 685–703. Simplifed equations of motion for the radial-axial vibrations of fluid filled pipes.
7. S. FINNVEDEN 1997 *Journal of Sound and Vibration* **199**, 125–154. Spectral finite element analysis of the vibration of straight fluid-filled pipes with flanges.
8. *ABAQUS Theory and User Manual* 1996 HKS Ltd.
9. C. A. FELIPPA 1988 *Communications in Applied Numerical Methods* **4**, 561–563. Symmetrization of coupled eigenproblems by eigenvector augmentation.
10. B. M. IRONS 1970 *AIAA Journal* **8**. Role of part-inversion in fluid–structure problems with mixed variables.
11. R. H. MACNEAL *et al.* 1980 *ASME Paper* 80-c2/*pvp*116. A symmetric modal formualtion of fluid-structure interaction, including a static approximation to higher order fluid modes.
12. C. H. HODGES, P. NASH and J. WOODHOUSE 1987 *Applied Acoustics* **22**, 47–69. Measurement of coupling loss factors by matrix fitting, an investigation of numerical procedures.
13. D. A. BIES and S. HAMID 1980 *Journal of Sound and Vibration* **70**, 187–204. In situ determination of loss and coupling loss factors by the power injection method.
14. K. D. LANGHE and P. SAS 1996 *Journal of the Acoustical Society of America* **100**, 291–303. Statistical analysis of the power injection method.
15. D. N. MANIK 1998 *Journal of Sound and Vibration* **211**, 521–526. A new method for determining coupling loss factors for SEA.
16. B. J. BREVART and C. R. FULLER 1996 *Journal of Sound and Vibration* **190**, 763–774, Energy exchange between the coupled media of impulsively excited, fluid-filled, elastic cylinders.
17. S. FINNVEDEN 1997 *Journal of Sound and Vibration* **208**, 705–728. Formulas for modal density and for input power from mechanical and fluid point sources in fluid filled pipes.
18. K. HERON 1996 *Philosophical Transactions of the Royal Society of London* **346**, 501–510. Advanced statistical energy analysis.
19. N. LALOR 1990 *ISVR Technical Report No*. 182. Considerations for the measurement of internal and coupling loss factors of complex structures.
20. F. J. FAHY 1998 *Journal of Sound Vibration* **214**, 261–267. An alternative to the SEA coupling loss factor: rational and method for experimental determination.